

Simple synthesis of nano-sized refractory metal carbides by combustion process

Hyung Il Won · Nersisyan Hayk · Chang Whan Won ·
Hyuk Hee Lee

Received: 7 February 2011 / Accepted: 12 April 2011 / Published online: 5 May 2011
© Springer Science+Business Media, LLC 2011

Abstract Combustion reactions of transition metal oxides (WO_3 , MoO_3 , Ta_2O_5 , Nb_2O_5 , ZrO_2 , and TiO_2), magnesium, carbon, and sodium fluoride produce a range of nanostructured transition metal carbides (W_2C , Mo_2C , TaC , NbC , ZrC , and TiC) with low amounts of free carbon. Sodium fluoride improves unfavorable combustion regimes and facilitates the carburization of metal carbides. The average particle size of carbides prepared in this study was below 100 nm in pure phase. The carbides were characterized by X-ray diffraction, scanning electron microscopy, specific surface area analysis, and carbon analysis.

Introduction

Carbides of transition metals in Groups IV–VI are widely used in the manufacture of cutting and drilling tools and wear-resistant parts in many types of machines because of their attractive properties such as high hardness, wear and erosion resistance, and stability at high temperatures [1, 2]. Recently, they have also been used as catalysts for manufacturing organic materials [3–5].

During the past two decades, substantial efforts have been devoted to synthesizing nano-sized carbide powders to obtain carbide materials with a nano-crystalline structure and considerably improved mechanical properties. Such

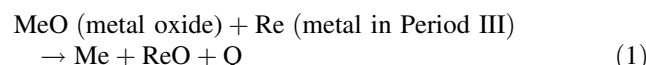
powders have two advantages. First, a nano-sized powder facilitates the formation of a nano-crystalline structure. Second, nano-sized carbide powders can be used easily to manufacture sophisticated micro devices such as micro-drills and micro-knives [6, 7].

Several researchers have used methods such as the conventional solid-state reactions [8–10], high-energy mechanical ball milling [11–13], spray conversion [14, 15], chemical vapor reactions [16, 17], and plasma-assisted vapor reactions [18, 19] to synthesize nano-sized carbide powders. These methods can be used to successfully form nano-sized carbide particles, but they present problems such as broad particle distribution, high impurity levels, and high-energy consumption and cannot be employed for mass production. Further, they do not yield high-quality carbide powders.

In this study, we employed the method of combustion synthesis (CS), also referred to as self-propagating high-temperature synthesis (SHS), for the synthesis of nano-sized transition metal carbide powders; this method holds promise as an efficient, energy-conserving technique for producing refractory carbides, borides, and many other compounds [20]. Metal oxides have been used in conjunction with Period III metals such as Na, Mg, and Al to synthesize carbides by CS, because the reaction between the metal oxides and the Period III metals produces sufficient amount of heat for carburization to occur [21, 22].

H. I. Won (✉) · N. Hayk · C. W. Won
Rapidly Solidified Materials Research Center (RASOM),
Chungnam National University, Yusung,
Daejeon 305-764, Korea
e-mail: rotc4379@hanmail.net

H. H. Lee
Korea Research Institute of Chemical Technology,
Daejeon 305-600, South Korea



Although this method offers the advantage of achieving carburization with a short, simple reaction, researchers have pointed out that it cannot be used to successfully form

nano-sized particles and achieve narrow particle distribution. In recent investigations, sodium chloride was used as a diluent reagent in CS, and it was found that this salt offers various advantages, e.g., it provides easy control of combustion temperature and facilitates diffusion [21, 22]. However, these investigation results still do not provide an efficient method for synthesizing nano-sized carbide powders.

Here, we report a simple preparation method of nano-sized transition metal carbide powders with excellent physical and chemical characteristics using CS.

Experimental

The raw materials used in this research were metal oxides, magnesium, carbon black, and sodium fluoride, all of which had greater than 98% purity. The particle size of the metal oxides ranged from 0.3 to 0.6 μm . The green mixture was ball milled with zirconia balls for 12 h and then stamped into a cylindrical mold with a diameter and height of 4–5 cm each. The prepared sample was placed in a combustion reactor, which was then sealed, evacuated, and filled with argon gas up to the desired pressure (2.5 MPa). An electrically heated nickel–chromium wire was used to initiate the combustion reaction, which was completed in a few minutes.

First, two tungsten–rhodium thermocouples (W/Re-5 vs. W/Re-20) were inserted into the reaction sample to record temperature profiles and to calculate the combustion temperature (T_c) and wave combustion (propagation) speed (U_c). The combustion speed was calculated as $U_c = x/t$. The t value is the time interval between the temperature profiles, and x is the distance between the thermocouples. A schematic diagram of the combustion reactor used in this study is shown in Fig. 1.

The by-products (sodium fluoride and magnesium oxide) of the combustion reaction were eliminated using

distilled water and hydrochloric acid. The final products were characterized using an X-ray diffractometer (Siemens, Germany, D-5000), a surface area analyzer (Micromeritics, U.S.A., ASAP 2010), and a field emission scanning electron microscope (FESEM; JEOL Japan, JSM 6330F). A carbon–sulfur determinator (ELTRA CS-800) was used to analyze free carbon concentration of the final products.

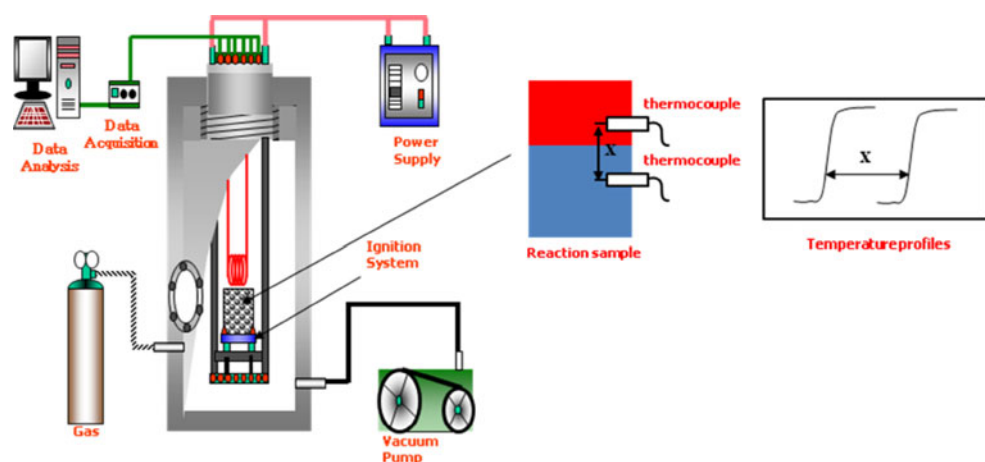
Result and discussion

The combustion reactions of binary and ternary metal oxides of Groups IV–IV with a stoichiometric concentration of magnesium and carbon (MeO (metal oxide) + Mg + C) are so highly exothermic that the combustion temperature of each reaction reaches more than 2000 °C. Although the temperatures and the amount of heat generated are theoretically sufficient to accomplish carburization as mentioned earlier, there are two significant problems in preparing nano-sized carbide particles via these combustion reactions: rapid particle growth and phase incompleteness. Table 1 shows that the reaction of $\text{MeO} + \text{Mg} + \text{C}$ reaches high combustion temperatures of >2100 °C and

Table 1 Products prepared from MeO (metal oxide) + Mg + C and its combustion characteristics

Reactants	T_c (°C)	U_c (cm/ s)	Particle size (μm)	Products after combustion and acid treatment
$\text{WO}_3 + 3\text{Mg} + 0.5\text{C}$	2800	2.5	>1.0	W, W_2C
$\text{MoO}_3 + 3\text{Mg} + 0.5\text{C}$	>3000	2.4	0.7–5.0	$\text{Mo}, \text{Mo}_2\text{C}$
$\text{Ta}_2\text{O}_5 + 5\text{Mg} + 2\text{C}$	2800	2.4	0.7–3.0	TaC, TaO
$\text{Nb}_2\text{O}_5 + 5\text{Mg} + 2\text{C}$	2800	2.4	0.5–5.0	$\text{Nb}_2\text{C}, \text{NbC}, \text{NbO}$
$\text{ZrO}_2 + 2\text{Mg} + 1\text{C}$	2000	2.0	>0.5	ZrC
$\text{TiO}_2 + 2\text{Mg} + 1\text{C}$	2400	2.5	1.0	TiC

Fig. 1 Schematic diagram of experimental apparatus



combustion speeds of >2.0 cm/s. Under these conditions, particles can grow quickly during the reaction; measurements of the powders from the $\text{MeO} + \text{Mg} + \text{C}$ reaction showed particle sizes of >500 nm. In addition, high combustion temperatures can easily result in the vaporization of Mg, which has a relatively low boiling point (1100 °C). The vaporized Mg leads to a high propagation speed, and some portion of vaporized Mg is vigorously released from the mixture sample; such strong gas release not only interferes with the diffusion between the reduced metal and carbon but also results in insufficient reduction of metals because of the low Mg concentration in the mixture sample. Therefore, it is difficult to realize complete carburization via the $\text{MeO} + \text{Mg} + \text{C}$ reaction, and the final products contain incomplete intermediate phases.

In order to solve the above mentioned problems, we used NaF as a diluent for CS. Figure 2 shows the combustion temperature and speed measured from the Me (metal oxide) + Mg + C + αNaF reactions. It was observed that an increase in the NaF concentration led to a decrease in the temperature in each combustion system. Further, each system showed different maximum concentrations of NaF which is a maximum capacity that can make propagation of the mixture (W_2C : 8 mol, Mo_2C : 8 mol, TaC : 9 mol, NbC : 10 mol, TiC : 2 mol, ZrC : 1.5 mol). This difference in the NaF concentrations is because of different exothermicities of the chemical interactions of different metals, i.e., Mg and C. For example, the calculated exothermicity of the Mo system, in which a maximum of 8 M of NaF can be introduced, was -265.22 kcal, whereas that of the Ti system was -105.87 kcal. The horizontal portion observed at $\alpha = 1-2$ corresponds to the phase transformation of NaF (from gas to solid). In addition, notably, the maximum concentration

of NaF is not the optimum condition to prepare single-phase carbide. This is because at the maximum concentration, the combustion temperature (reaction temperature) is too low for complete carburization.

Table 2 shows the combustion characteristics and phase composition of final products prepared from $\text{MeO} + \text{Mg} + \text{C} + \alpha\text{NaF}$. The NaF concentrations of each system listed in the table are optimized according to the amount of heat generated from each system and the phase composition of the final products. With the addition of appropriate amounts of NaF, the combustion temperature and particle propagation speed were considerably decreased to within the range of $1150-1350$ °C and $2.0-2.5$ cm/s, respectively. From these data, it can be conjectured that the combustion regime, once stabilized with NaF, corresponded to steady-state combustion with no strong gas release. During combustion, NaF was absorbed and considerable amount of the generated heat was used up as it was transformed into a liquid, with the result that the combustion temperature of the reaction was reduced to about 1200 °C. Mg did not vaporize at this temperature.

Figure 3 shows the FESEM micrograph of acid-treated products obtained from CS. FESEM, BET, and XRD calculation results, obtained using the Scherrer formula ($r = 0.9\lambda/B\cos\theta$), are listed in Table 2. These results show that the average particle size of the prepared carbide powders decreased to $20-100$ nm, and that every carbide powder had uniform spherical particles and a narrow particle size distribution. This change in particle size was mainly attributed to the low combustion temperature achieved by introducing NaF. The FESEM images of W_2C synthesized from the $\text{WO}_3 + 3 \text{Mg} + 0.5\text{C} + \alpha\text{NaF}$ system, shown in Fig. 4, support the size-reduction effect of NaF. As seen in this figure, the average particle size of W_2C decreased from 2 to $0.1\mu\text{m}$ with the increase in the NaF concentration. As mentioned above, an increase in NaF concentration causes a decrease in combustion temperature (reaction temperature), and the decreased reaction temperature slows down particle growth after the formation of metal carbide nuclei.

In addition to decreasing the combustion temperature and stabilizing the combustion regime, NaF showed another advantageous effect from the standpoint of carbide synthesis: it facilitated diffusion. The carburization from the MeO (metal oxide) + Mg + C mixture was mainly a result of solid-state diffusion. Because of the nature of CS and the rapid cool-down of the combusted sample, the diffusion time available for carburization was just $1.0 \sim 30$ s. With such a short reaction time, it is difficult to realize complete carburization, even at high combustion temperatures.

The introduction of NaF enabled the synthesis of a single phase (Table 2); the diffusion between metal and

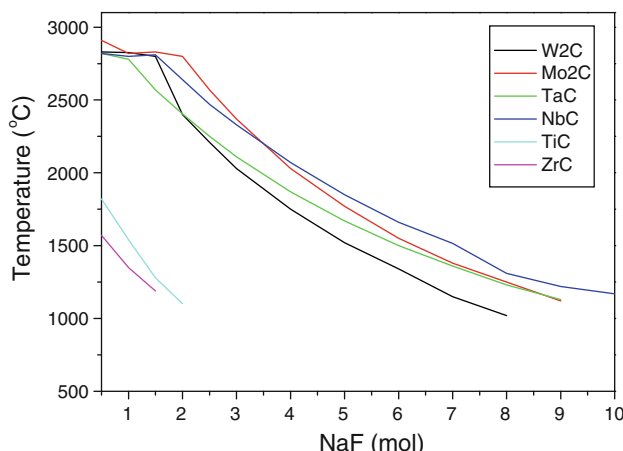
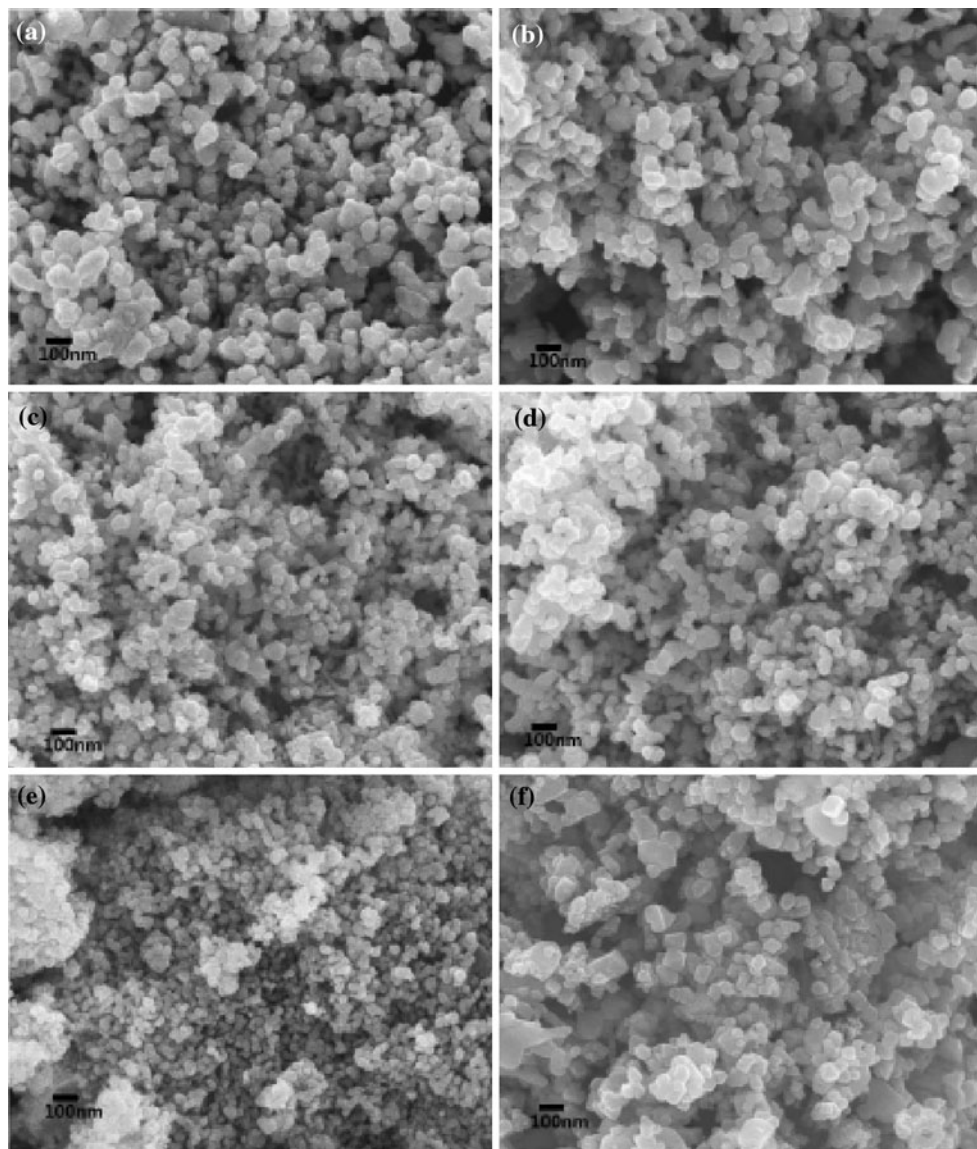


Fig. 2 Dependencies of T_c and U_c on the amount of NaF at combustion of MeO (metal oxide) + Mg + C + αNaF mixture; $P_{\text{Ar}} = 2.5$ MPa

Table 2 Products prepared from MeO (metal oxide) + Mg + C + NaF and its combustion characteristics

Reactants	T_c (°C)	U_c (cm/s)	Calculated particle size from XRD (nm)	BET (m^2/g)	Free carbon (%)	Products after acid treatment
$\text{WO}_3 + 3\text{Mg} + 0.5\text{C} + 7.0\text{NaF}$	1150	0.1	29	9.964	0.13	W_2C
$\text{MoO}_3 + 3\text{Mg} + 0.5\text{C} + 7.0\text{NaF}$	1250	0.17	37	12.754	0.05	Mo_2C
$\text{Ta}_2\text{O}_5 + 5\text{Mg} + 2\text{C} + 8.0\text{NaF}$	1200	0.06	27	10.856	0.04	TaC
$\text{Nb}_2\text{O}_5 + 5\text{Mg} + 2\text{C} + 8.0\text{NaF}$	1210	0.05	42	19.124	0.07	NbC
$\text{ZrO}_2 + 2\text{Mg} + \text{C} + 1.3\text{NaF}$	1280	0.17	18	45.576	0.05	ZrC
$\text{TiO}_2 + 2\text{Mg} + \text{C} + 1.5\text{NaF}$	1310	0.1	31	17.759	0.03	TiC

**Fig. 3** SEM micrograph of the acid-treated products from combustion of MeO (metal oxide) + Mg + C + NaF mixture: **a** W_2C , **b** Mo_2C , **c** TaC, **d** NbC, **e** ZrC, and **f** TiC

carbon was facilitated by the liquid-phase NaF that was formed during combustion. Figure 5 shows the X-ray diffraction (XRD) pattern of acid-treated products obtained

from CS. Indexing the powder patterns showed that cubic metal carbide was formed in the case of TaC, NbC, ZrC, and TiC and that hexagonal W_2C and orthorhombic Mo_2C

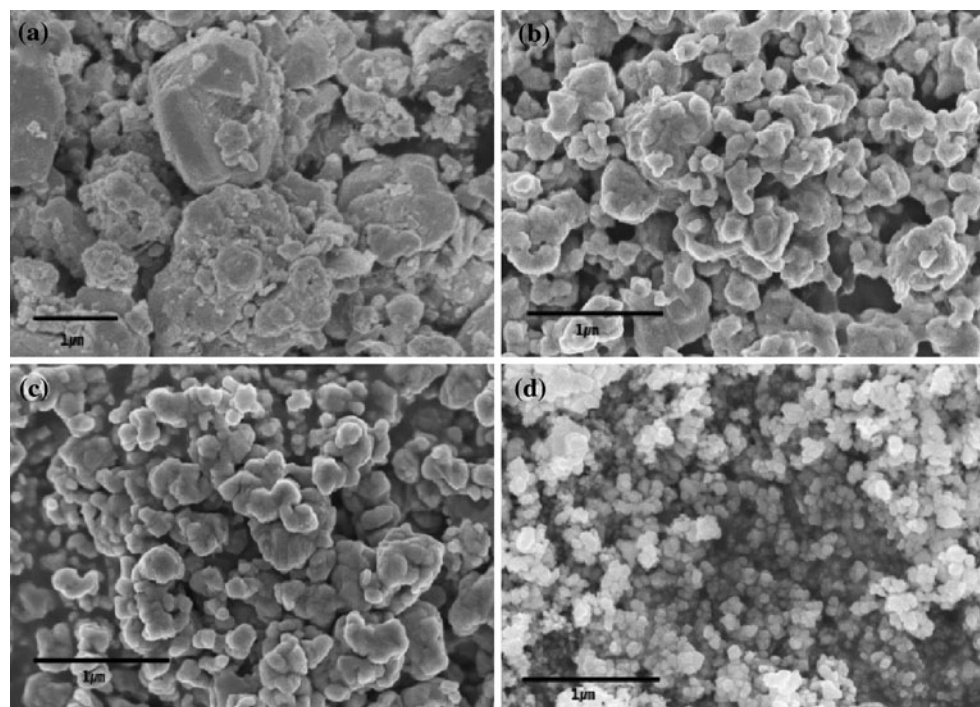


Fig. 4 Microstructure of tungsten carbide powders synthesized from the mixture of $\text{WO}_3 + 3\text{Mg} + 0.5\text{C} + x\text{NaF}$: **a** $\alpha = 2.0$, **b** $\alpha = 4.0$, **c** $\alpha = 6.0$, and **d** $\alpha = 8.0$

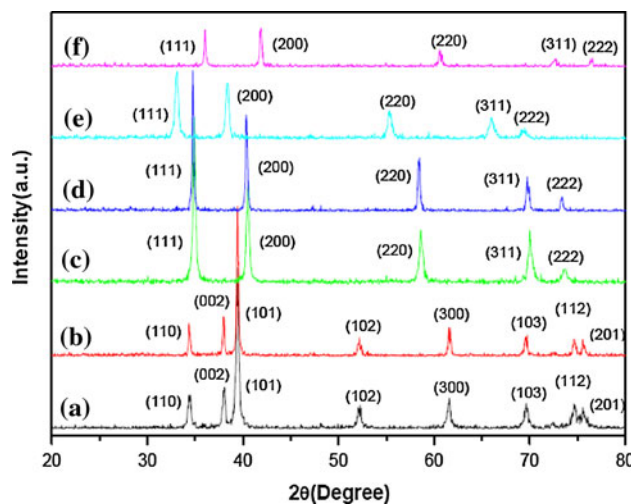


Fig. 5 X-ray powder diffraction pattern of the acid-treated products from combustion of MeO (metal oxide) + $\text{Mg} + \text{C} + \text{NaF}$ mixture: (a) W_2C , (b) Mo_2C , (c) TaC , (d) NbC , (e) ZrC , and (f) TiC

were also formed. In addition, the low concentration of free carbon indicated that the combustion reaction from the $\text{MeO} + \text{Mg} + \text{C} + \text{NaF}$ mixture has a high degree of conversion when forming transition metal carbides, as shown in Table 2.

In the former investigations of CS for carbides (WC and TiC), the alkali salt used was generally sodium chloride [22, 23]. NaCl is suitable for providing single-phase

carbides but not for the preparation of nano-sized carbide particles with narrow particle distribution because it has a limit to decrease combustion temperature. Figure 6 shows that the average particle size of WC and TiC powders synthesized from the NaCl system were 1.0 and 0.3 μm , respectively. According to former investigations, for TiC, the maximum concentration of NaCl that can be introduced into the initial mixture was 0.58 mol and the combustion temperature in this condition was higher than 1700 °C, which was too high to allow the formation of nano-sized particles. On the other hand, up to 2.0 mol of the NaF system could be introduced and a low combustion temperature of up to 1100 °C could be reached under this condition. The reason for this result in maximum introducing concentration and low combustion temperature can be attributed to the fact that the melting temperature of NaCl is lower than that of NaF (NaCl melting point: 800 °C; NaF melting point: 1000 °C). When an alkali salt is used as a diluent for CS, the maximum concentration that can be introduced into the initial mixture is small when the melting temperature of the salt is low as compared to that when the melting temperature is high. This phenomenon can be understood from the reaction sequence of the $\text{MeO} + \text{Mg} + \text{C} + \text{NaF}$ mixture. The general description of the reaction sequence is shown in Fig. 7.

When the combustion reaction begins to propagate along the electric filament and the temperature of the mixture reaches 600 °C, solid Mg starts to melt (Zone A).

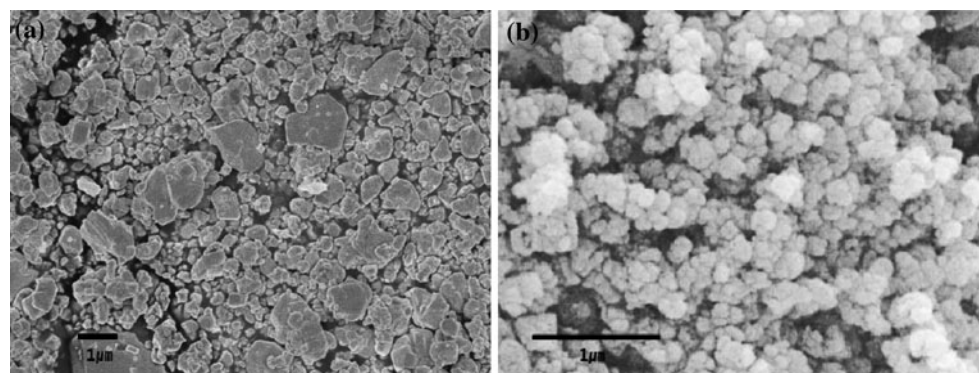


Fig. 6 Carbide powders synthesized from NaCl system : **a** WC and **b** TiC

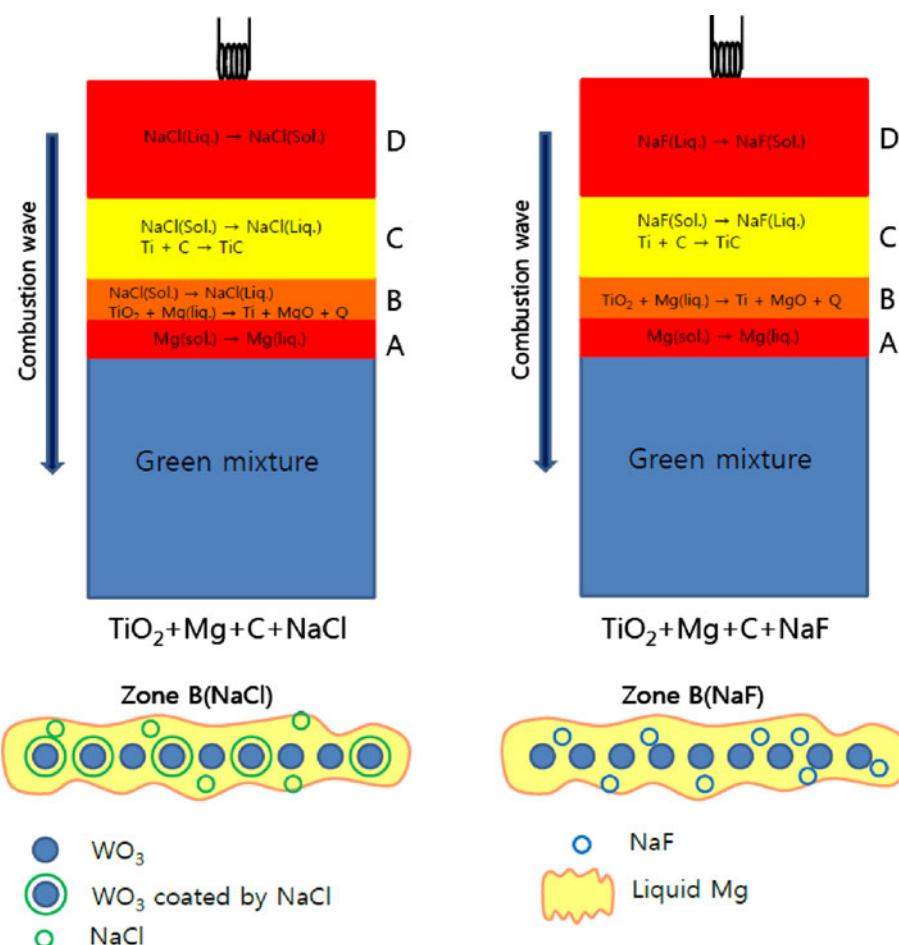


Fig. 7 Reaction sequence during the combustion synthesis

As it melts, Mg reacts with MeO to cause reduction in Zone B. In this zone, heat is produced from the reduction reaction between MeO and Mg and the temperature of the mixture increases to the melting point of NaCl or NaF. Here, because the temperature of the mixture increases in an instant, some amount of NaCl starts to melt quickly. As it melts, it blocks the reduction reaction by covering MeO

particles before the melted Mg can reach them. Therefore, higher the quantity of NaCl introduced, greater will be the extent of blocking of the reduction reaction. However, NaF melts slowly and requires long time to cover the MeO particles because of its high melting point, so that the quantity of NaF that can be introduced in the mixture is larger than that of NaCl. Consequently, alkali salts with

low melting points show a limited capacity in decreasing the combustion temperature.

Conclusion

We have demonstrated that self-propagating SHS is not restricted to producing nanostructured carbide powders. The reactions between a range of metal oxides, magnesium, and carbon in the presence of sodium fluoride offer an efficient, effective method for producing a range of transition metal carbides. Sodium fluoride improves unfavorable combustion regimes and facilitates the carburation of metal carbide. The reaction of the $\text{MeO} + \text{Mg} + \text{C} + \text{NaF}$ mixture yields nano-crystalline materials in the required temperature range of 1100–1300 °C with low combustion speeds of 0.05–0.2 cm/s.

References

1. Storms EK (1967) The refractory carbides. Academic Press, New York
2. Toth LE (1971) Transition metal carbides and nitrides. Academic Press, New York
3. Hyeon T, Fang M, Suslick KS (1996) J Am Chem Soc 118:5492
4. Izhar S, Yoshida M, Nagai M (2009) Electrochim Acta 54:1255
5. Katharine P, Jun L, Robert S, Holly NS, Zhang J, Judith KS et al (2008) Solid State Sci 10:1499
6. Fang ZZ, Wang X, Ryu T, Hwang KS, Sohn HY (2009) Int J Refract Met Hard Mater 27:288
7. Carroll DF (1999) Int J Refract Met Hard Mater 17:123
8. Wang HM, Wang XH, Zhang MH, Du XY, Li W, Tao KY (2007) Chem Mater 19:1801
9. Hanif A, Xiao T, York APE, Sloan J (2002) Chem Mater 14:1009
10. Nartowski AM, Parkin IP, Mackenzieb M, Craven AJ (2001) J Mater Chem 11:3116
11. Fecht HJ (1992) Nanostruct Mater 1(2):125
12. Fecht HJ, Hellstern E, Fu Z, Johnson WL (1990) Metall Mater Trans A 21(9):2333
13. Porat R, Berger S, Rosen A (1996) Mater Sci Forum 225–227(Pt 1):629
14. Seegopal P, Gao L (2003) US pat 6 524 366
15. Zhang ZY, Wahlberg S, Wang MS, Muhammed M (1999) Nanostruct Mater 12(1–4):163
16. Swihart MT (2003) Curr Opin Colloid Interface Sci 8(1):127
17. Kim JC, Kim BK (2004) Scr Mater 80:969
18. Fukumasa O, Fujiwara T (2003) Thin Solid Films 435:33
19. Tong LR, Reddy RG (2005) Scr Mater 52:1253
20. Alexander GM (2004) J Mater Chem 14:1779
21. Won HI, Nersisyan HH, Won CW (2008) J Mater Res 23:2393
22. Nersisyan HH, Lee JH, Won CW (2003) Mater Res Bull 38:1135
23. Nersisyan HH, Lee JH, Won CW (2002) J Mater Res 17:2859